



Adsorption layer and flow within liquid meniscus in forced dewetting

V. I. Kovalchuk¹ and G. K. Auernhammer²

Abstract

In surfactant solutions, the bulk hydrodynamic flow couples to extensional/compressional surface flows due to Marangoni stresses induced at the interface. With the increasing surfactant concentration, these Marangoni stresses can suppress the surface flows and lead to non-moving, retarded, surfaces. We review this phenomenon with special focus on the dynamic dewetting of a substrate pulled out of a pool of surfactant solution. In this case, the dewetting meniscus surface can be retarded (fully or partially) because of the appearance of surface tension gradients opposing the flow in the adjacent liquid. With an increasing flow velocity, the non-uniformity of the meniscus surface becomes stronger resulting in its separation on a mobile and an immobile part with a sharp transition between them. The presence of a non-uniform adsorption layer at the meniscus surface strongly complicates the dewetting dynamics which becomes dependent on the surfactant balance at the surface.

Addresses

¹ Ovcharenko Institute of Biocolloid Chemistry, Kyiv (Kiev), 03142, Ukraine

² Leibniz-Institut für Polymerforschung Dresden e.V., Dresden, Germany

Corresponding author: Kovalchuk, V.I. (vladim@koval.kiev.ua)

Current Opinion in Colloid & Interface Science 2023, 67:101723

This review comes from a themed issue on **Wetting and Spreading (2023)**

Edited by **Tatiana Gambaryan-Roisman** and **Victor Starov**

For a complete overview see the [Issue](#) and the [Editorial](#)

<https://doi.org/10.1016/j.cocis.2023.101723>

1359-0294/© 2023 The Author(s). Published by Elsevier Ltd. This is an open access article under the CC BY license (<http://creativecommons.org/licenses/by/4.0/>).

Keywords

Dynamic adsorption layer, Surfactant solution, Marangoni effect, Surface retardation, Forced dewetting, Dynamic contact angle.

Introduction

Surface active substances are omnipresent in the nature and technological processes [1–5]. These are substances such as low molecular weight surfactants, polymers, lipids, proteins, and so on. Due to their high surface activity, they tend to accumulate in interfacial layers, modifying their properties. Highly surface-active

amphiphilic substances, like long-chain fatty acids or phospholipids, can adsorb at the interfaces in large amounts even though they are present in negligible amounts in the bulk of liquids [6–8]. Special procedures are required to purify liquids from surfactants.

Surfactants (in a broad sense — surface active agents) play an important role in many technological and daily household processes, such as the generation of foams and emulsions, deposition of coating films, multiphase flows, froth flotation, printing, micro- and nano-fluidic processes, washing and cleaning, and so on. [1,2,9–13]. In such processes, interfacial adsorption layers act often under highly dynamic conditions. Viscous stresses and pressure variations, arising in solutions, influence the interfacial layers and drive them out of equilibrium. As a consequence, various relaxation processes can be initiated within the adsorption layers, such as adsorption or desorption of the molecules, accompanied by diffusion relaxation, reorientation and change of conformation of the adsorbed molecules, formation or break up of molecular aggregates and complexes, formation and change of a structure within the layers, Marangoni flows and others [14–19]. Such adsorption layers under non-equilibrium conditions (called also dynamic adsorption layers [20]) are a subject of numerous experimental and theoretical studies.

Additionally, interfacial adsorption layers themselves can strongly influence the dynamics of liquid systems. Surfactants can modify the bulk properties of liquids (viscosity, density) if they are present in sufficiently large amounts. But much more important effect is the modification of the interfacial properties (interfacial tension, interfacial visco-elasticity) by surfactants, even if they are present in rather small amounts [21]. Interfacial properties are included in normal and tangential stress boundary conditions. Through the boundary conditions, surfactants influence the dynamic behavior of the whole system, if it contains free fluid/liquid interfaces [21–23].

Consequently, there is a coupling between hydrodynamic processes and physicochemical processes in liquid systems containing surfactants. Hydrodynamic flows distort the surfactants distributions within the system and the interfacial layer properties. This results in the appearance (or modification) of gradients in the surface tension

and capillary pressure jumps, i.e. in normal and tangential forces applied to the liquid at its interfaces, resulting in changes in the flow pattern. There is a feedback between the hydrodynamics of the systems and the dynamics of the surfactant adsorption layers. In many cases, by sufficiently large deviations from the equilibrium, such a feedback can lead to instabilities of the system, like in the case of spontaneous surface tension oscillations [24,25] or meniscus oscillations in Langmuir wetting processes [26]. Understanding the mechanisms of such complex processes and describing or modeling them theoretically is a challenge for fluid dynamics and interfacial science because hydrodynamic and physicochemical processes interact in a complex way with each other.

Wetting menisci are another example of systems where hydrodynamics and physical chemistry are strongly interconnected. There are two alternative approaches to describe the wetting/dewetting dynamics of pure liquids. One of them is based on the analysis of hydrodynamic energy dissipation within the three-phase contact zone [27,28]. Another approach focuses on the kinetics of the molecular processes determining the value of the microscopic contact angle [29,30]. Several combined approaches are also proposed [30] (and references therein). Extensive experimental and theoretical studies were performed to approve the proposed approaches [31], but the description of the wetting/dewetting dynamics even for pure liquids remains semi-empirical and not complete [30,32] even though new approaches combining molecular dynamics simulations and the above modeling approaches give promising new insights [33–35].

In practical cases, however, one deals mostly not with simple pure liquids but rather with multi-component mixtures (solutions), containing very often surface-active species. Though there were attempts to describe the wetting dynamics also for the case of surfactant solutions [36–39], the problem remains much less studied than the case of pure liquids. The main difficulty in the solution of the problem arises due to the coupling between the hydrodynamic and physicochemical processes, as discussed above. The region near the three-phase contact line is characterized by very strong velocity gradients and significant viscous stresses acting at the fluid/liquid interface [40]. They disturb the adsorbed surfactant layer at the meniscus surface. It is supposed that even in the case of pure liquids, the interfacial layers should be disturbed near the contact line [30,41–44]. This is more the case for surfactant solutions [17].

The properties of dynamic adsorption layers have been widely studied for other surfactants containing systems, where also a mutual influence of hydrodynamic flows and adsorption layers takes a place under the similar conditions. These are such systems like bubbles and drops rising (falling) or growing in surfactant solutions

[20,22,45–49], thin liquid films [50–52], capillary waves [22,53], liquid-infused surfaces [54], and others. A detailed analysis of such systems was presented recently in the study by Manikantan and Squires [21]. These studies are very useful for the analysis of the adsorption layers behavior under specific dynamic conditions in wetting. In particular, the studies of bubbles and drops rising or falling in surfactant solutions point out at a strongly non-uniform distribution of the surfactants adsorbed at their interfaces [47,48,55–57]. The resulting interfacial tension gradients, opposing the flow in the adjacent liquid, strongly influence the local velocity profiles and the terminal velocities of the bubbles and drops, which become dependent on the surfactant type and concentration [58–60] (and references therein). In such systems, the non-uniformity of the surfactant distribution at the interface reveals itself in the formation of a fully retarded zone (so-called stagnant cap) at the rear of the moving bubble or drop [61–64], i.e. a zone in which the surface tension gradients fully suppress surface flows. A sharp transition between a mobile and fully retarded zone at the interface is often observed in the case of impurities collected on the upstream side of an obstacle, at the leading edge of a spreading oil slick or in other similar systems [65] (and references therein).

In a stationary state, one should expect that strongly non-uniform dynamic adsorption layers form also at the surface of wetting/dewetting menisci of surfactant solutions. The meniscus surface can be retarded (fully or partially) because of the appearance of surface tension gradients opposing the flow in the adjacent liquid, i.e. because of the Marangoni stresses at the surface. There are observations, which support the hypothesis that Marangoni stresses close to the contact line can be responsible for the sharp decrease of dynamic receding contact angles [17,66]. The calculation of the flow characteristics in the meniscus becomes much more challenging in the presence of non-uniform adsorption layers because it requires to consider the surfactant transfer in the bulk and at the surface and its adsorption/desorption.

The present paper is aimed to analyze the effect of non-uniform dynamic adsorption layers on the flow within steady dewetting menisci. To this end, we combine the results for the wetting dynamics with those for other liquid systems where dynamic adsorption layers play a significant role. Such approach gives a new look at the problem allowing a deeper understanding of the details of the processes accompanying the dynamic wetting/dewetting in surfactant systems and helping in the modeling of this complicated phenomenon.

Experimental investigations of steady dewetting processes

The analysis of dynamic adsorption layers at liquid interfaces is much simpler for steady flow conditions,

when the liquid velocity and surfactants distributions do not change with time. Therefore, we present here the experimental method of rotating horizontal cylinder partially immersed in a surfactant solution (Figure 1) [66–70]. The advantage of this method is the possibility of a continuous observation of advancing or receding contact angles during a sufficiently long time after a steady state is established. It allows to study the forced wetting regimes over a wide range of wetting/dewetting speeds (10^{-4} to 1 m/s). Also, the equilibrium and dynamic contact angles can be controlled by making the surface of the cylinder more hydrophobic or more hydrophilic with a controlled roughness, depending on the conditions of a particular experiment. Accordingly, the experimental setup is suitable for the studies of the contact angle hysteresis, which can appear due to surface roughness, chemical heterogeneity of the surface, as well as due to specific interaction between the substrate surface and the air/water interface in a close vicinity of the triple contact line [31].

Precise dependencies of the dynamic contact angles on the velocity of the moving surface (or capillary number) can be obtained with this instrument by analyzing side-view images taken with a high-speed camera. The experiments can be performed under controlled temperature and humidity conditions. The flow profiles within the setup can be visualized by adding small amounts of particles dispersed in the liquid. The particle movement, observed with another high-speed camera, can be analyzed by using the particle tracking plugin of ImageJ [66].

In the study by Henrich et al. [66], the dynamic receding contact angles were measured with the rotating cylinder setup for several surfactants of different type and solubility. This included anionic (sodium 1-decanesulfonate,

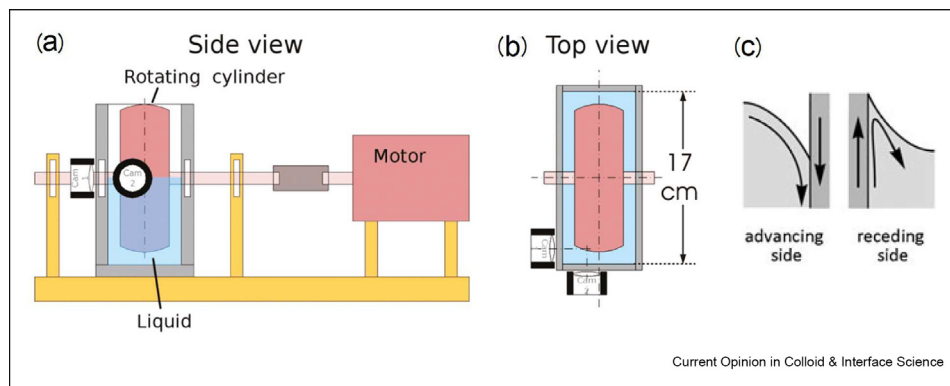
S-1DeS), cationic (cetyltrimethylammonium bromide, CTAB), and non-ionic surfactants (oxyethylated alcohols C4E1, C8E3 and C12E5). The results are presented in Figure 2.

Typical dynamic receding contact angle *versus* velocity dependencies are shown in Figure 2a. At velocities larger than 10 mm/s, the experimental data are in a good agreement with the hydrodynamic theories by Voinov [71] and Cox [27] (solid lines) and by Eggers [72] and Chan et al. [73] (dashed lines), respectively. For lower velocities, the molecular or the combined molecular–hydrodynamic theory [30,74] is usually more appropriate. It was suggested recently in the study by Butt et al. [75] that the low velocity part of the dependencies can be explained by an adaptation (i.e. relaxation) of the dewetted substrate surface. Such adaptation should depend on the substrate material properties and its interaction with the liquid.

The dynamic contact angle *versus* velocity curves, shown in Figure 2a, strongly depend on the surfactant concentration in the solution. Both the apparent receding contact angles for zero velocity and the critical velocity, corresponding to zero contact angles, decrease with the surfactant concentration increase. In Figure 2b, the dynamic contact angle *versus* surfactant concentration dependencies at a velocity of 6 mm/s are shown. They also demonstrate the effect of the surfactant type and concentration on the dynamic contact angle.

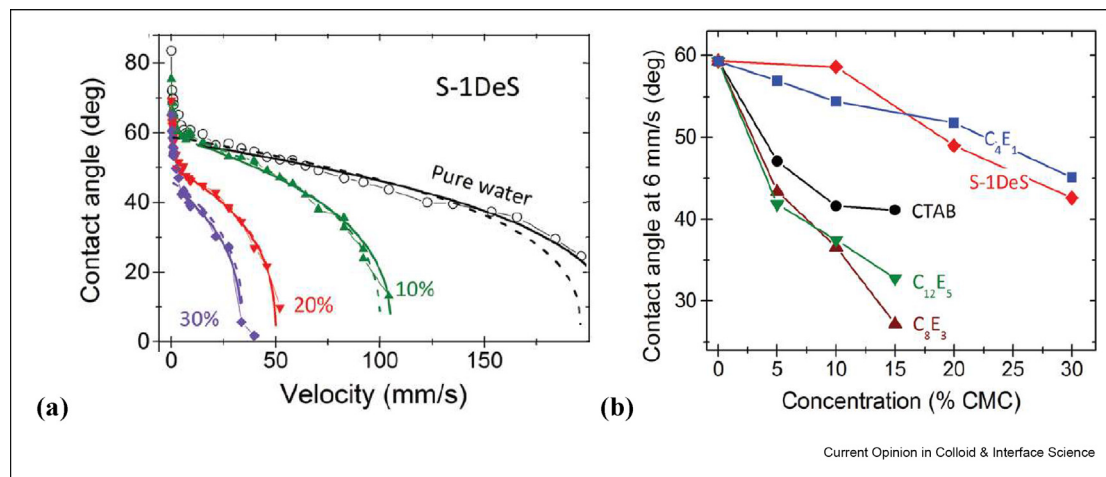
The critical micelles concentration (CMC) values for the considered surfactants span between $7.0 \cdot 10^{-2}$ and $1.2 \cdot 10^3$ mM, i.e. over more than four orders of magnitude [66]. This means that the diffusion kinetics should be also very different for these surfactants due to the strongly varying characteristic diffusion distances [17].

Figure 1



Schematic of the experimental setup: (a) and (b) the side and top views of the rotating cylinder setup, (c) sketch of the hydrodynamic flow close to the advancing and receding contact lines. Reprinted (adapted) with permission from *Langmuir* 27, 2112(Copyright 2011, American Chemical Society) [67] and *Colloid Polym Sci* 291, 361(Copyright 2012, Springer Verlag) [68].

Figure 2



Dynamic receding contact angle of aqueous solutions of S-1DeS versus velocity (a) and dynamic receding contact angles at a velocity of 6 mm s^{-1} versus surfactant concentration (in % of CMC) for the surfactants CTAB (cationic), S-1DeS (anionic), and C₄E₁, C₈E₃, C₁₂E₅ (non-ionic) (b) on a polystyrene-coated cylinder (adapted from the study by Henrich et al. [66]). The solid and dashed lines in (a) are fits using the hydrodynamic theories as discussed in the text. The surfactants concentrations (in % of CMC) are shown at the curves (Soft Matter, 2016, 12, 7782- Published by The Royal Society of Chemistry). CMC, critical micelles concentration.

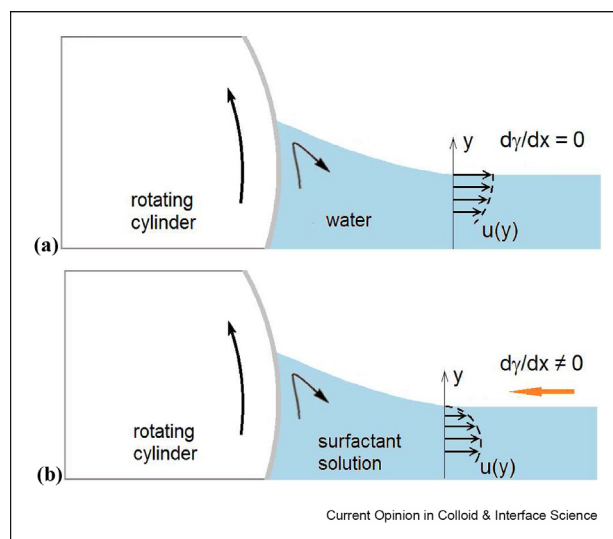
It is remarkable, however, that the effect of the surfactant type on the dynamic contact angle is not so significant as it could be expected from the difference in the CMC values. Moreover, there is no clear correlation between the CMC values and the effect of the surfactant type on the dynamic contact angle. Thus, though the diffusion kinetics is important for the dynamic contact angle variation with the velocity, the effect of other possible factors should be also considered. One such factor is the surfactant distribution over the surface, which depends strongly on the velocity distribution in the solution near the surface and not exclusively on the adsorption kinetics. In this case, the experimental observations give strong indications that the effects change when surfactant can be transported over the liquid surface from the receding contact line to the advancing contact line [17,68]. In the following, we consider situations in which the dynamics of each contact line can be dealt independently, i.e. we neglect effect discussed in the study by Straub et al. [17] and Fell et al. [68].

Here, two limiting situations should be considered. In pure water (or a very diluted surfactant solution), the surface tension practically does not change and the water layer is mobile. For a receding meniscus, the water layer at the surface moves away from the meniscus, driven by the viscous flow produced by the rotating cylinder in the bulk of water (Figure 3a). The water surface is continuously expanded in the vicinity of the contact line. If traces of a surfactant are present at the surface, they are swept from the meniscus surface

toward the vessel wall. Near the vessel wall, in contrast to the meniscus, the water surface is continuously contracted; therefore, the surfactant traces can accumulate here and desorb into the bulk of water.

The situation is completely different in the case of a surfactant solution, if its concentration is sufficiently high. The surfactant molecules adsorbed at the surface can support the surface tension gradients, which

Figure 3



Rotating cylinder in contact with pure water (a) and a surfactant solution (b).

counteract the viscous flow close to the surface. As a result, at sufficiently high surfactant concentrations, the solution surface becomes almost completely immobile (Figure 3b). These two situations are very similar to the behavior of bubbles rising in surfactant solutions. In pure water, the bubble surface is free of surfactants and mobile, and the rising velocity is high, while in surfactant solutions, the surface of bubbles is immobilized by adsorbed molecules, and the rising velocity becomes much smaller [58,59].

In intermediate cases, the situation is more complex. If the solution surface is not completely immobile, the surfactant molecules adsorbed at the surface are swept from the meniscus surface toward the vessel wall. The intensity of convection decreases fast with increasing distance from the rotating cylinder surface. Therefore, the adsorption layer is only slightly disturbed by the flow far away from the meniscus. This means that the surface tension is not very different from the equilibrium one, γ_{eq} , at the remote parts of the surface. At the meniscus surface, the adsorbed molecules are swept, and the surface tension is larger than equilibrium one. However, it cannot be larger than that for pure water, γ_0 . Hence, the maximum possible total surface tension difference over the solution surface is close to the surface pressure, $\Pi = \gamma_0 - \gamma_{eq}$, for this particular surfactant concentration. The higher the surfactant concentration, the larger is the surface pressure and the stronger are surface tension gradients, counteracting the viscous flow at the surface.

The equilibrium surface tension and surface pressure of different surfactants depend on their adsorption activity. Usually, they are functions of the dimensionless ratio c/a , where c is the surfactant concentration and a is the adsorption equilibrium constant, reflecting its surface activity (a smaller constant a means a higher surface activity). The equilibrium constant a increases with the CMC increase and, for air/water interface, it is usually by about one order of magnitude smaller than CMC [76]. This means that if the concentrations of two surfactants in % of CMC are similar, then their ratios c/a should be also similar. In this case also, the equilibrium surface tensions and surface pressures of these surfactant solutions should be similar. Accordingly, the surface tension gradients, counteracting the viscous flow at the surface, should be not very different for such two solutions at similar flow velocities. This can be a possible explanation why the results obtained in the study by Henrich et al. [66] for surfactants with very different CMC values are not very different (Figure 2b).

Theoretical approaches

Governing equations

The velocity distribution \mathbf{u} within the solution can be obtained from a set of Navier–Stokes equations

$$\rho \frac{\partial \mathbf{u}}{\partial t} + \rho \mathbf{u} \cdot \nabla \mathbf{u} = -\nabla p + \mu \Delta \mathbf{u} \quad (1)$$

and the continuity equation for an incompressible liquid

$$\nabla \cdot \mathbf{u} = 0 \quad (2)$$

where p is the pressure, ρ and μ are the density and dynamic viscosity of the solution. The surfactant distribution in the solution volume is described by the convective diffusion equation

$$\frac{\partial c}{\partial t} + \mathbf{u} \cdot \nabla c = D \Delta c \quad (3)$$

where c and D are the concentration and diffusion coefficient of the surfactant in solution. The surfaces are assumed to move parallel to itself, i.e. the normal velocity components are zero at the surfaces. For the rotating cylinder surface, we will assume here a non-slip boundary condition

$$\mathbf{u} = \mathbf{U} \quad (4)$$

where \mathbf{U} is the velocity vector at the cylinder surface. The non-slip condition is not valid for a small region near the contact line of the order of distances where typical surface forces are acting (i.e. below 100 nm) [40]. However, our consideration here concerns much larger distances, where Eq. (4) is valid.

The boundary condition for the solution surface represents the tangential stress balance

$$\frac{\partial \mathbf{u}_t}{\partial n} = -\frac{1}{\mu} \nabla_s \gamma \quad (5)$$

where \mathbf{u}_t is the tangential velocity component near the surface, n is the coordinate normal to the surface, γ is the surface tension, and ∇_s is the surface gradient operator.

If the interfacial layer is under local equilibrium conditions, the local surface tension is a function of adsorption (surface concentration) Γ . This function is given by a specific equation of state for the surfactant $\gamma = \gamma(\Gamma)$. The adsorption Γ can be obtained from the dynamic surfactant balance at the surface, which is given by the equation [21,22].

$$\frac{\partial \Gamma}{\partial t} + \nabla_s (\Gamma \mathbf{u}_s - D_s \nabla_s \Gamma) + D \left(\frac{\partial c}{\partial n} \right)_s = 0 \quad (6)$$

where D_s is the surface diffusivity of the surfactant and \mathbf{u}_s is the surface velocity. The second term in Eq. (6) describes the surfactant redistribution within the interfacial layer due to surface convection and diffusion. The last term is

the surfactant flux between the interfacial layer and subsurface solution. At the substrate (cylinder) surface, the adsorbed surfactant moves with the surface and the surface diffusion can be neglected

$$\frac{\partial \Gamma}{\partial t} + \nabla_s(\Gamma U) + D \left(\frac{\partial c}{\partial n} \right)_s = 0 \quad (7)$$

Under dynamic conditions, the adsorption Γ should be related to the bulk surfactant concentration close to the surface, c_s (subsurface concentration). If a kinetic adsorption barrier is absent, then local adsorption equilibrium can be assumed, and the required relationship is given by the respective adsorption isotherm equation $\Gamma = \Gamma(c_s)$ for each of the surfaces. If there is an adsorption barrier, then the respective kinetic adsorption equation should be applied [20,55–57,60].

To complete the formulation, one has also to include the conditions at the contact line (or at the border of a small region near the contact line, excluded from the consideration) and within the bulk solution far away from the contact line (or at the vessel walls, if the actual geometry is considered). The initial conditions are not necessary, if steady-state regimes are considered. For this case, the terms with time derivatives disappear from Eqs. (1), (3), (6), and (7).

It is seen that Eqs. (3) and (5)–(7) set a coupling between the hydrodynamic and physicochemical variables. Therefore, in a general case, the hydrodynamic and convective diffusion equations should be solved together, what can be a complicated task. We will use here a simplified approach presuming certain surfactant distribution for the solution surface.

The dimensionless variables can be introduced as follows: $\tilde{t} = \frac{U}{L}t$, $\tilde{\mathbf{u}} = \frac{\mathbf{u}}{U}$, $\tilde{p} = \frac{L}{\mu U}p$, $\tilde{c} = \frac{c}{c_{eq}}$, $\tilde{\Gamma} = \frac{\Gamma}{\Gamma_{eq}}$, $\tilde{\gamma} = \frac{\gamma}{RT\Gamma_{eq}}$, where L is the characteristic length (it can be chosen in different ways), $U = |\mathbf{U}|$ is the substrate velocity, c_{eq} and Γ_{eq} are the equilibrium surfactant concentration and adsorption, and R , T , and Γ_{eq} are the gas constant, absolute temperature, and limiting adsorption, respectively. Then the dimensionless form of Eqs. (1)–(7) will be

$$\text{Re} \left(\frac{\partial \tilde{\mathbf{u}}}{\partial \tilde{t}} + \tilde{\mathbf{u}} \cdot \tilde{\nabla} \tilde{\mathbf{u}} \right) = -\tilde{\nabla} \tilde{p} + \tilde{\Delta} \tilde{\mathbf{u}} \quad (8a)$$

$$\tilde{\nabla} \tilde{\mathbf{u}} = 0 \quad (8b)$$

$$\frac{\partial \tilde{c}}{\partial \tilde{t}} + \tilde{\mathbf{u}} \cdot \tilde{\nabla} \tilde{c} = \frac{1}{Pe} \tilde{\Delta} \tilde{c} \quad (8c)$$

$$\tilde{\mathbf{u}} = \tilde{\mathbf{U}} \quad (8d)$$

$$\frac{\partial \tilde{u}_t}{\partial \tilde{n}} = -Ma \tilde{\nabla}_s \tilde{\gamma} \quad (8e)$$

$$\frac{\partial \tilde{\Gamma}}{\partial \tilde{t}} + \tilde{\nabla}_s(\tilde{\Gamma} \tilde{u}_s) - \frac{1}{Pe_s} \tilde{\Delta}_s \tilde{\Gamma} + \frac{N_E}{Pe} \left(\frac{\partial \tilde{c}}{\partial \tilde{n}} \right)_s = 0 \quad (8f)$$

$$\frac{\partial \tilde{\Gamma}}{\partial \tilde{t}} + \tilde{\nabla}_s(\tilde{\Gamma} \tilde{\mathbf{U}}) + \frac{N'_E}{Pe} \left(\frac{\partial \tilde{c}}{\partial \tilde{n}} \right)_s = 0 \quad (8g)$$

In Eqs. (8a)–(8g), the following dimensionless numbers appear: the Reynolds number $Re = \rho UL/\mu$, the Péclet and surface Péclet numbers $Pe = UL/D$ and $Pe_s = UL/D_s$, the Marangoni number $Ma = RT\Gamma_{eq}/\mu U$, and the two numbers $N_E = c_{eq}L/\Gamma_{eq}$ and $N'_E = c_{eq}L/\Gamma_{eq}$, characterizing the adsorption activity of the surfactant at the liquid and substrate surface, respectively (sometimes called “exchange numbers”). The Marangoni number is defined here in a usual way [55–57,60,62,64].

Solutions for fully mobile and fully retarded air/liquid interface

Two important limiting cases should be considered first. They are related to the situations when the air/liquid interface is either free of surfactants or is fully retarded by the adsorbed surfactants. In the former case, the surface tension gradients are absent and the viscous stresses are zero at the surface, according to Eq. (5). In the latter case, the surface tension gradients are so high that the flow velocity at the surface turns to zero. In these two cases, the solution of the hydrodynamic problem can be obtained separately from the convective diffusion problem.

We will consider here liquid flow in a wedge formed by two flat surfaces, one of which is a solid surface moving with a constant velocity parallel to itself and another one is a liquid surface, either free of surfactants and mobile or motionless due to the presence of surfactants (Figure 4). The situation with a flat meniscus surface can be easily realized in the rotating cylinder device by filling the liquid in the vessel up to the level, where the angle formed between the liquid surface and the cylinder surface is equal to the dynamic contact angle for the given contact line velocity. For the distances from the contact line much smaller than the cylinder radius, the cylinder surface can be approximately considered as locally flat. We consider here a 2D flow structure, which is realized only for long cylinders in the vertical symmetry plane perpendicular to the horizontal cylinder axis, equidistant from the cylinder bases. With

increasing distance from this plain, the third velocity component becomes more and more significant.

The velocity distributions for the flow in such wedge geometry were obtained by Moffatt [77], who has considered the case of small Reynolds numbers and solved the Stokes equation, neglecting the left part of Eq. (1) (or Eq. (8a)).

Then, for the first case of *zero viscous stresses* at the liquid surface, the velocity components in the plane polar coordinates (r, θ) can be obtained as

$$u_r = U \frac{\sin \phi \cos(\phi - \theta) + \theta \sin \phi \sin(\phi - \theta) - \phi \cos \theta}{\phi - \cos \phi \sin \phi} \tag{9}$$

$$u_\theta = U \frac{\phi \sin \theta - \theta \sin \phi \cos(\phi - \theta)}{\phi - \cos \phi \sin \phi} \tag{10}$$

where $U = |U|$ is the velocity of the dewetting solid surface which is inclined in the liquid at the angle ϕ . The substrate velocity $u_r(r, 0) = -U$, i.e. it is negative when the substrate leaves the liquid. U has to be replaced by $-U$ when the substrate moves in the opposite direction.

For the second case of *zero velocity* at the liquid surface, the velocity components are the following

$$u_r = U \frac{\phi \sin \theta - \phi(\phi - \theta)\cos \theta + \sin \phi \sin(\phi - \theta) - \theta \sin \phi \cos(\phi - \theta)}{\phi^2 - \sin^2 \phi} \tag{11}$$

$$u_\theta = U \frac{\phi(\phi - \theta)\sin \theta - \theta \sin \phi \sin(\phi - \theta)}{\phi^2 - \sin^2 \phi} \tag{12}$$

Eqs. (11) and (12) describe the so-called Taylor scraping flow [78]. Further developments of this theory can be found, e.g. in the study by Kuhlmann et al. [79] and Mahmood et al. [80].

In Eqs. (9)–(12), the polar angle θ changes between 0 (at the solid surface) and ϕ (at the liquid surface) (Figure 4). The radial coordinate r changes in the theoretical limits from infinitely small to infinitely large values. For this case, the additional boundary conditions at the contact line and within the bulk solution far away from the contact line are not necessary.

We emphasize that in the both solutions, Eqs. (9)–(10) and (11)–(12), the flow velocity does not depend on the radial coordinate r , i.e. on the distance to the contact

line. This is possible, provided the velocity at both wedge surfaces do not change with the radial coordinate, as in the two considered cases. The color diagrams for the velocity distributions given by Eqs. (9)–(12) are shown in Figure 4.

From the velocity distributions in Eqs. (9)–(12), the viscous stresses and pressure distributions can be obtained. In the case of a free solution surface, the viscous stresses and pressure are the following

$$P_{r\theta} = P_{\theta r} = \frac{2\mu U}{r} \cdot \frac{\sin \phi \sin(\phi - \theta)}{\phi - \sin \phi \cos \phi} \tag{13}$$

and

$$p = p_0 + \frac{2\mu U}{r} \cdot \frac{\sin \phi \cos(\phi - \theta)}{\phi - \sin \phi \cos \phi} \tag{14}$$

For an immobile solution surface, the viscous stresses and pressure are given by

$$P_{r\theta} = P_{\theta r} = \frac{2\mu U}{r} \cdot \frac{\phi \cos \theta - \sin \phi \cos(\phi - \theta)}{\phi^2 - \sin^2 \phi} \tag{15}$$

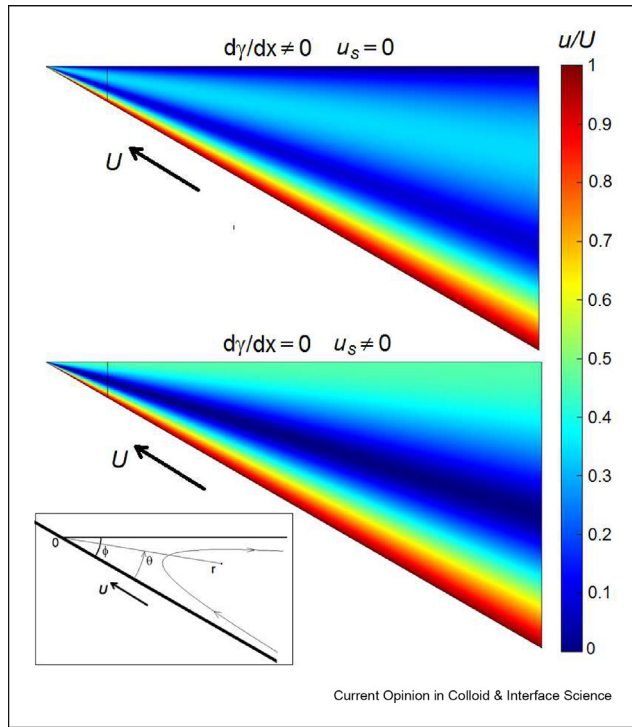
and

$$p = p_0 + \frac{2\mu U}{r} \cdot \frac{\phi \sin \theta + \sin \phi \sin(\phi - \theta)}{\phi^2 - \sin^2 \phi} \tag{16}$$

where p_0 is a constant external pressure.

As can be seen from Eqs. (13)–(16), the viscous stresses and pressure distributions are inversely proportional to the distance from the contact line r . This leads to a singularity at the contact line because both the viscous stresses and pressure increase without bound here. This problem is intensively discussed in the related literature. To avoid the viscous stresses singularity, the non-slip boundary condition, Eq. (4), should be modified, when the distance between the substrate and the liquid surface becomes small — of the order of characteristic length for surface forces action [27,30,40]. Also, the pressure increase near the contact line leads to deformations of the meniscus surface. Hence, the surface curvature effect should be accounted for [27,28,37–39].

Figure 4



Velocity distributions in a plane wedge with one steadily moving and one free (bottom) or motionless (top) flat surfaces. The velocity distributions are self-similar for all distances. For definiteness, the overall distance along the upper surface shown here is 8 mm. The black vertical line marks the distance 1 mm from the contact line (cf. Figure 5). The inset shows the polar co-ordinate system (r, θ) .

However, such very small distances are not the subject of the present study; therefore, we do not consider these effects in details here.

It has been shown by Moffatt that for the velocity distributions considered here, the Reynolds number should increase with the distance from the contact line as $Re \sim \rho U r / \mu$ because the distance r is the only characteristic length in absence of other characteristic lengths. For $U = 10$ cm/s, $r = 1$ mm, and $\nu = \mu / \rho = 10^{-6}$ m²/s, this gives $Re \sim 100$. Thus, the Reynolds numbers are not small for the distances of order 1 mm. Nevertheless, the numerical solutions of the full Navier–Stokes equations showed that they are very close to the Moffatt solutions, Eqs. (9)–(12), for this particular flow structure (Figure S2 in Supplementary Information). The difference between inertial and non-inertial flow behavior in a wedge was analyzed recently in the study by Mahmood and Siddiqui [80]. The so-called ‘Reynolds ridge’ often observed at the transition region of surface-contaminated liquids is a phenomenon of finite and large Reynolds numbers. Under Stokes flow conditions, the air/liquid interface should be considered as a flat surface [65].

Surface tension gradients at the immobile part of the surface

The Moffatt solutions presented above can be used to analyze the surface tension gradients at the solution surface immobilized by surfactants. The viscous stresses are zero at a free solution surface ($\theta = \phi$), according to Eq. (13), as this was prescribed by the boundary conditions for this case. For an immobile-surface solution, the viscous stresses are not zero at $\theta = \phi$. For this case, one obtains from Eqs. (5) and (15)

$$P_{r\theta}(r, \phi) = -\frac{2\mu U}{r} \cdot \frac{\sin \phi - \phi \cos \phi}{\phi^2 - \sin^2 \phi} = \frac{d\gamma}{dr} \quad (17)$$

To keep the solution surface immobile, the surface tension gradient should balance the viscous stresses. With decreasing distance to the contact line, the surface tension gradient should increase as the viscous stresses are increasing. Integrating Eq. (17), one can obtain the difference of the surface tensions between two arbitrary points at the surface, r_1 and r_2 , as

$$\Delta\gamma = \gamma_2 - \gamma_1 = 4.6\mu U F(\phi) \cdot \lg \frac{r_1}{r_2} \quad (18)$$

where $F(\phi) = \frac{\sin \phi - \phi \cos \phi}{\phi^2 - \sin^2 \phi}$ is a function, depending on the dynamic contact angle ϕ . For small contact angles this function behaves as $F(\phi) \sim \phi^{-1}$. However, it is of the order of unity for contact angles between 45° and 75° (decreases from 1.3 to 0.8 between these two angles) and is about 2 for a contact angle of 30°.

Eqs. (17) and (18) express the force balance at a flat meniscus surface for a steady-state dewetting process. In particular, Eq. (18) shows that, to keep the surface immobile, the surface tension should decrease with a constant decrement $-4.6\mu U F(\phi)$, when the distance to the contact line increases by one order of magnitude. For a substrate velocity $U = 10$ cm/s, viscosity $\mu = 10^{-3}$ Pa s and a dynamic contact angle $\phi = 60^\circ$ the decrement should be of about -0.46 mN/m, and on a distance varying by six orders of magnitude ($r_2 / r_1 = 10^6$), the surface tension difference should consist of about 2.76 mN/m. The dimensionless form of Eq. (18) is

$$\Delta\tilde{\gamma} = \tilde{\gamma}_2 - \tilde{\gamma}_1 = \frac{4.6F(\phi)}{Ma} \cdot \lg \frac{r_1}{r_2} \quad (19)$$

Thus, the dimensionless surface tension decrement depends on the Marangoni number as $-4.6F(\phi)/Ma$. The smaller is Marangoni number, i.e. the larger is the velocity U , the faster is the surface tension decrease. The decrement increases with decreasing dynamic contact angle ϕ .

As it was discussed above, in real systems for large distances from the contact line, the surface tension should not be very different from the equilibrium one, γ_{eq} . At the same time, the surface tension near the contact line cannot be larger than that for pure solvent, γ_0 . Therefore, the surface tension difference over the meniscus surface cannot exceed the value of about $\Pi = \gamma_0 - \gamma_{eq}$. Accordingly, the dynamic adsorption layer can keep the surface immobile, while the surface tension difference required to balance the viscous stresses does not exceed the maximum possible surface tension difference for the given surfactant concentration in the solution: $\Delta\gamma \leq \Pi(c)$. If the flow velocity increases so, that $\Delta\gamma$ exceeds Π , then the dynamic adsorption layer is unable to balance the viscous stresses further and should start to move away from the contact line. By adding surfactant to the solution, we can increase the surface pressure Π and restore the force balance at the surface.

It is instructive to compare the flow in a dewetting meniscus with the flow around bubbles rising in surfactant solutions (or drops of heavier liquids falling in solutions) [47,48,55–64]. The viscous stresses at the bubble surface produce surface tension gradients counteracting the flow and reducing the bubble rising velocity. The higher is the flow velocity, the stronger are the gradients. However, the surface tension difference between the bubble top and bottom is limited. The surface tension at the bubble top cannot be higher than that for pure solvent, γ_0 . And the surface tension at the bubble bottom cannot be significantly smaller than the equilibrium one, γ_{eq} , because the excess of surfactant continuously desorbs from the bottom. When the surface tension difference required to balance the viscous stresses exceeds the maximum possible surface tension difference, the bubble surface cannot remain immobile anymore. In such situations the upper part of the bubble surface becomes mobile, whereas an immobile “stagnant cap” remains at the lower part [47,48,55–64].

The situation with splitting of the surface of liquid containing surfactant traces onto mobile and immobile part due to viscous flow in the bulk is not unique. The similar situation can be observed, for example, in liquid films flowing on a solid substrate with impurities collected on the upstream side of an obstacle, at the leading edge of a spreading oil film or at liquid-infused surfaces in the presence of surfactants (see Refs. [54,65,81] and references therein). For liquid menisci the possibility of formation of surfactant free regions under dynamic conditions on the surface of surfactant containing liquids was considered, in particular, by Cox [36] and by Chesters et al. [37,38].

The situation in dewetting menisci is rather similar to bubbles rising in surfactant solutions. The submillimeter or millimeter size of rising bubbles is similar to the typical liquid menisci size. Additionally, the typical

bubble rising velocities (from some mm/s to tens of cm/s) are of the same order of magnitude, as the flow velocities within dewetting menisci. Therefore, one can expect that also the viscous stresses and surface tension gradients are of the same order of magnitude for the considered two situations.

Thus, if the surfactant concentration in solution, c , and the respective surface pressure, $\Pi(c)$, are sufficiently small, whereas the flow velocity is high, the surface tension difference required to balance the viscous stresses, $\Delta\gamma$, can exceed the maximum possible surface tension difference for this solution concentration, approximately equal to $\Pi(c)$. In this case, similarly to the situation with rising bubbles, a part of the meniscus surface located closer to the contact line can become mobile. The surfactant molecules can adsorb here, but due to surface flow, they should be continuously moved away from the contact line. The surface layer at this meniscus part is continuously expanded, and the surfactant concentration should remain small here. Therefore, the surface tension should be close to that for pure solvent, γ_0 , and the viscous stresses should be close to zero. But further away from the contact line the surface velocity decreases, and, accordingly, the surface layer at the respective part of the surface should be continuously compressed. The surfactant concentration should be much higher here, than at the mobile part of the surface, and, therefore, the developed surface tension gradients opposing the flow can be sufficient to immobilize this part.

Flow in a plane wedge with partially immobilized surface

The studies on rising bubbles and falling drops show that the transition between the mobile and immobile parts of the surface can be rather sharp [21,47,48,55–57,61–63,65]. This allows one to use an idealized, so-called, stagnant cap model, where one part of the surface is assumed to be completely mobile, whereas the other part is completely immobile. In this case, the hydrodynamic problem also can be solved separately from the convective diffusion problem, as in the case of Moffatt solution. The presence of surfactants is revealed only through the dependence of the size of the immobile part on the surfactant concentration and adsorption kinetics. To solve the hydrodynamic problem, one can consider the size of the immobile part as an additional system parameter.

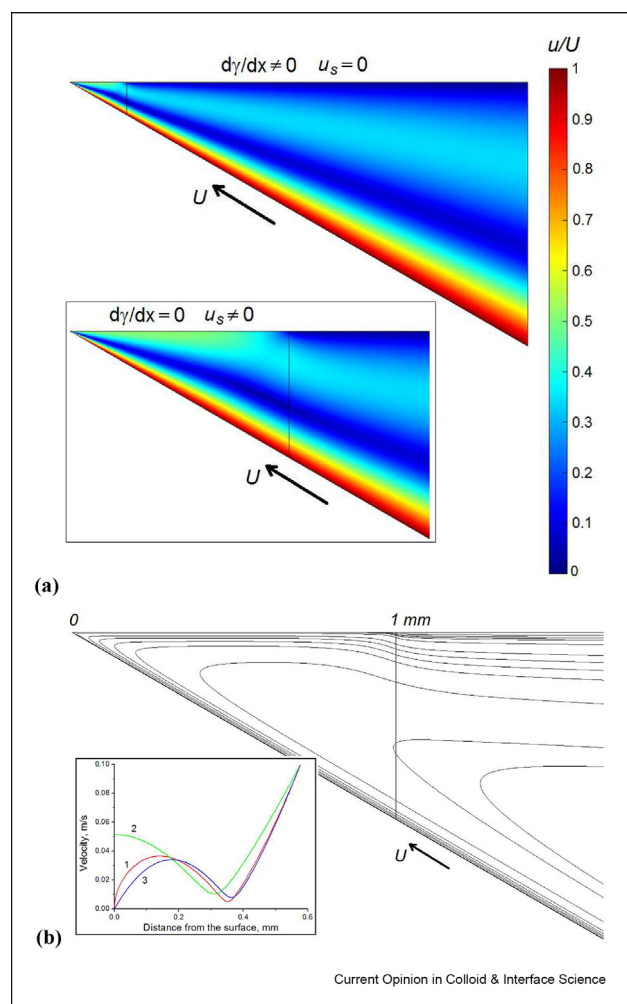
Such approach gives a solution for the flow in a plane wedge sufficiently far from the transition region between the mobile and immobile parts of the surface, but it ignores the details of the flow and surfactant concentration distribution close to the transition region. For a close vicinity of this region, another solution can be found which asymptotically matches with the ‘outer’ solution [65]. However, even with this simplification,

the hydrodynamic problem remains rather complicated and has no simple analytic solution because the surface velocity strongly depends on the distance in this case, in contrast to the Moffatt solution. To avoid mathematical complications, it is convenient, similarly to the case of rising bubbles, to solve the problem numerically.

In Figure 5, one can see the velocity distribution in a plane wedge, where a part of the surface near the contact line ($r < r_0$) is completely mobile, whereas the remaining part ($r > r_0$) — completely immobile. The solution can be obtained under the assumption of zero viscous stresses at the mobile part and zero surface velocity at

the immobile part. The computational domain in this particular case is limited by flat vertical planes (or also cylindrically shaped borders) at the distances $0.5 \mu\text{m}$ and 8 mm from the contact line. For these two borders, the velocity distributions given by the respective Moffatt solutions can be used as the boundary conditions, i.e. Eqs. (9) and (10) for $r = 0.5 \mu\text{m}$ and Eqs. (11) and (12) for $r = 8 \text{ mm}$. The point separating the mobile and immobile parts (marked by a black vertical line in Figure 5) is chosen here at the distance $r_0 = 1 \text{ mm}$ from the contact line. The external borders at the distances $0.5 \mu\text{m}$ and 8 mm are located sufficiently far from this point, what allows to use the respective Moffatt solutions there. Figure 5b shows the flow lines in the wedge.

Figure 5



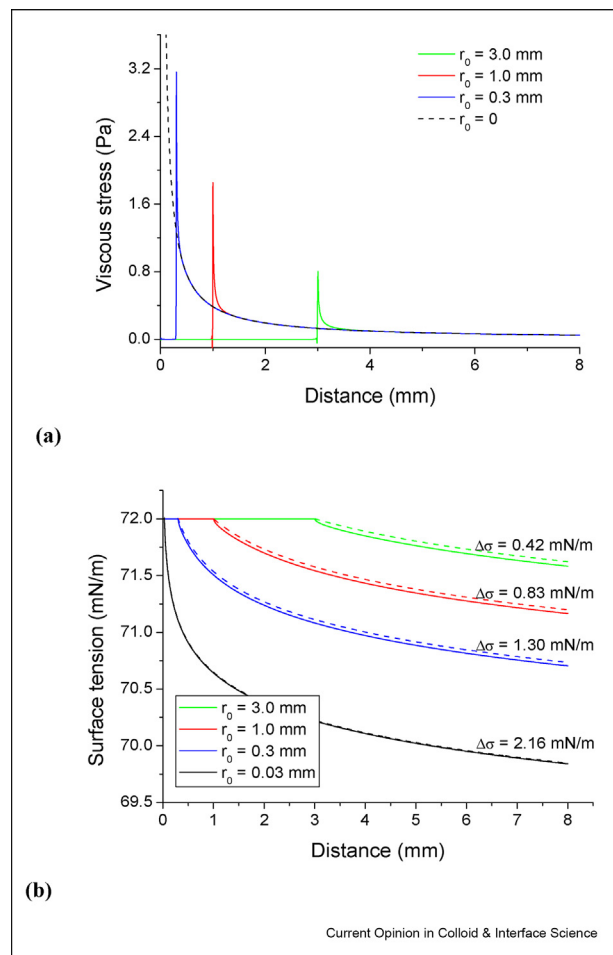
Velocity distribution (a) and flow lines (b) in a plane wedge with one steadily moving flat surface and one surface composed of a mobile and an immobile part. The computational domain is limited by flat vertical planes at the distances $0.5 \mu\text{m}$ and 8 mm from the contact line. The thin vertical line marks the border between the mobile and immobile part of the solution surface at the distance 1 mm from the contact line (cf. Figure 4). The inset in (a) is a zoom of the part closest to the contact line. The inset in (b) shows the velocity profiles in the vertical cross-section along the thin vertical line (the solution surface is composed of a mobile and an immobile part (1), is completely mobile (2) or completely immobile (3)).

As it is seen from Figure 5, the velocity distributions sufficiently far left and right from the point separating the mobile and immobile parts of the surface resemble those for free and motionless flat surfaces, shown in Figure 4 (bottom and top, respectively). Close to the border between the mobile and immobile parts, we have a transition velocity distribution. Close to the contact line, the maximum velocity in the liquid flowing back from the contact line is located at the surface, but with increasing distance, it moves to the bulk to go around the retarded part of the surface. The surface velocity is initially large and almost constant near the contact line, but it decreases fast when the flow approaches the leading edge of the retarded part and turns to zero after this border.

The velocity components in the bulk also sharply change in the transition region near the border between the mobile and immobile part at the solution surface. This leads to a sharp increase of the viscous stresses in this region, as it is shown in Figure 6a. Such sharp increase of the viscous stresses at the leading edge of a stagnant cap is also a typical feature of bubbles/drops rising/falling in surfactant solutions [47,48,55,56]. It is seen from Figure 6a that the height of the peaks increases with a decreasing distance to the contact line. But after the peaks, the viscous stresses approach fast those for a completely retarded surface, given by Eq. (17), because the respective velocity distributions become very similar with increasing distance. The viscous stress peaks presented in Figure 6a are very sharp as we assumed here a negligibly small transition region between the mobile and immobile part of the surface. In a real experimental system, the peaks should be not so sharp, as soon as there will be a transition region with a small but finite width, which is determined by surfactant surface diffusion and adsorption from the bulk (see below subsection *Surfactant balance at the surface*).

When the tangential viscous stress distributions are known, they can be integrated over the surface, according to Eq. (5), and the surface tension distributions

Figure 6



Viscous stresses (a) and surface tension (b) distributions within the immobile part of the surface for different distances between its leading edge and the contact line: $r_0 = 3.0, 1.0, 0.3,$ and 0.03 mm; the dynamic contact angle $\phi = 30^\circ$; the substrate velocity $U = 10$ cm/s. Dashed line in (a) is the viscous stresses distribution at a completely retarded surface given by Eq. (17). Dashed lines in (b) are the surface tension distributions calculated by using Eq. (18). The surface tension differences over the shown distance (8 mm) are given at the respective curves.

can be obtained. Figure 6b shows the surface tension distributions for the mobile and immobile parts of the surface for several positions of the border of the immobile part with respect to the contact line. Within the mobile part, the surface tension remains constant and equal to the surface tension of pure solvent (water in this case). The surface tension begins to decrease at the beginning of the immobile part. The closer is the contact line to the immobile part, the larger is the surface tension difference over the surface, which is necessary to keep the surface layer immobile. The dashed lines show the surface tension distributions calculated by using Eq. (18) for the respective distances to the contact line. Eq. (18) gives the same logarithmic

decrement of the surface tension decrease, as the numerical solution, except of very small distances from the edge of the immobile part, where the viscous stresses sharply increase (cf. Figure 6a). Integration of the sharp viscous stresses peak at the beginning of the immobile part gives an initial surface tension decrease not accounted for by Eq. (18); therefore, the numerically calculated surface tension distributions run slightly below the respective curves obtained by using Eq. (18). However, this difference becomes less significant, when the immobile part begins closer to the contact line.

Thus, to keep the surface layer immobile, a respective surface tension difference within the surface layer is necessary. Figure 6b gives the examples of such surface tension differences over the distance of 8 mm for the specified parameters of the system. If the required surface tension difference exceeds the maximum possible difference for a given surfactant concentration, then the whole surface layer cannot remain immobile, and a mobile part appears near the contact line. The size of the mobile part increases, when the maximum possible surface tension difference decreases, as it is illustrated in Figure 6b.

For larger distances than shown in Figure 6b, the surface tension should continue to decrease with the same logarithmic decrement, but the respective additional contribution to the overall surface tension difference should be small, as the viscous stresses are very small here. Note also that the wedge geometry considered here is only a good approximation for the region near the contact line. For usual experimental conditions, where the meniscus rises up above a flat part of the solution surface in the vessel, the contribution of the flat part to the overall surface tension difference should be negligibly small, because the distance between the solution surface and the moving substrate surface increases by orders of magnitude compared to the meniscus region. Therefore, practically, all surface tension difference should be created over the meniscus surface only, i.e. over the distance of the order of capillary length $\lambda_C = \sqrt{\gamma_{eq}/\rho g}$, whereas within the flat part of the solution surface, the surface tension should remain close to the equilibrium one. For the rotating cylinder, its surface can be approximately considered as a locally flat, only if the distance to the contact line is much smaller than the cylinder radius. Further away from the contact line, the curvature of the cylinder surface becomes significant. Therefore, also in this case, the viscous stresses should decrease much faster with the distance than for a wedge with two plane surfaces, and practically, all surface tension difference should be created over the distances much smaller than the cylinder radius.

For very small (sub-micrometer) distances from the contact line, the application of the considered simplified hydrodynamic model is not completely correct, as

discussed above; therefore, the logarithmic surface tension decrement should be different here. However, both the meniscus surface deformation due to local hydrodynamic pressure increase and the possible slip at the substrate surface should lead to a decrease of the viscous stresses at the solution surface compared to the case of a plane wedge with no-slip boundary condition for the substrate surface. In this case, the logarithmic surface tension decrement should also not be significantly larger than that given by Eq. (18).

Thus, for not very small dynamic contact angles and not very viscous solutions, the overall surface tension difference produced by the viscous stresses within dewetting menisci should be of the order of several mN/m. The surface pressure at the solution surface can change from zero for a pure (or slightly contaminated) solvent up to several tens of mN/m at high surfactant concentrations, close to CMC. Thus, for high surfactant concentrations, the surface pressure can be much larger than the surface tension difference required to immobilize the surface layer. In this case, the meniscus surface will be completely immobile. However, if the surfactant concentrations are small (much smaller than CMC), so that the surface pressure is not sufficiently large to counteract the tangential viscous stresses at the surface, then the surfactant will be swept from a part of the surface.

Lubrication approximation

The analysis can be simplified if we use the lubrication approximation [82]. This approximation is usually used to describe velocity profiles between two surfaces, which have a small slope with respect to each other. It can be applied to the flow in dewetting menisci, if the dynamic contact angle ϕ is small. Following this approach, a simple equation can be obtained estimating the size of the free part of the meniscus surface (Eq. (S8) in *Supplementary Information*):

$$x_0 = \lambda_C \exp\left(-\frac{\Pi\phi}{2\mu U}\right) \quad (20)$$

For pure water in the absence of surfactants $\Pi = 0$, and this equation gives $x_0 = \lambda_C$, i.e. the whole meniscus surface is mobile. In the presence of a surfactant $\Pi \neq 0$, $x_0 < \lambda_C$, and the meniscus surface has a mobile part, for $0 < x < x_0$, and an immobile part, for $x_0 < x < \lambda_C$. The size of the mobile part, x_0 , decreases with increasing surface pressure, i.e. with increasing surfactant concentration in the bulk. In contrast, with the increasing substrate velocity, U , the size of the mobile part increases. The distance x_0 increases also with increasing viscosity and decreasing dynamic contact angle.

For $U = 10$ cm/s, $\phi = 0.1$, and $\mu = 1$ mPa s one obtains $2\mu U/\phi \approx 2$ mN/m. Thus, for these particular parameters, an increase of the surface tension difference by 2 mN/m should correspond to a decrease of the mobile part by a factor of e . It should be noted, however, that the dynamic contact angle and the capillary length also depend on surface tension; therefore, the effect of surface tension should be more complicated.

With the dimensionless equilibrium surface pressure $\tilde{\Pi} = \frac{\Pi}{RT\Gamma_\infty}$ Eq. (20) takes the form

$$x_0 = \lambda_C \exp\left(-\frac{Ma\tilde{\Pi}\phi}{2}\right) \quad (21)$$

When either Marangoni number or surface pressure $\tilde{\Pi}$ is zero, then there is no tangential stress at the whole meniscus surface ($x_0 = \lambda_C$). With increasing Marangoni number and surface pressure the effect of the surface tension gradient opposing the flow at the surface becomes stronger, and the size of the mobile part, x_0 , decreases. Smaller dynamic contact angle, ϕ , leads to higher tangential stresses and, therefore, to larger x_0 .

With $r_1 = \lambda_C$, $r_2 = r_0$, and $\Delta\gamma = \Pi$ Eq. (19) takes a similar form

$$r_0 = \lambda_C \exp\left(-\frac{Ma\tilde{\Pi}}{2F(\phi)}\right) \quad (22)$$

Eqs. (21) and (22) show that the size of the mobile part decreases exponentially with increasing surface pressure and increasing Marangoni number.

As it was discussed above, the hydrodynamic pressure within the solution increases with decreasing distance to the contact line. This pressure increase should lead to deformations of the surface of liquid. Then the Laplace pressure compensates the pressure difference between the liquid and air. According to Eq. (14), near a mobile surface ($\theta = \phi$), the pressure distribution is given by

$$p - p_0 = \frac{2\mu U}{r} \cdot \frac{\sin \phi}{\phi - \sin \phi \cos \phi} \quad (23)$$

The hydrodynamic pressure increase should be equal to the local capillary pressure $p_C = \gamma_0/R_C$, where R_C is the curvature radius. Then, it follows from Eq. (23) that the curvature radius increases with the distance to the contact line

$$R_C = \frac{r}{2Ca} \cdot \frac{\phi - \sin \phi \cos \phi}{\sin \phi} \quad (24)$$

where $Ca = \mu U/\gamma_0$ is the capillary number. For large distances, the curvature radius is large and the curvature effect can be neglected. However, the curvature effect can be significant at small distances to the contact line. For $U = 10$ cm/s, $\mu = 10^{-3}$ Pa s, and $\gamma_0 = 70$ mN/m, the capillary number is about $Ca \sim 1.5 \cdot 10^{-3}$. Thus, the curvature radius is large compared to the distance for all distances, and the capillary pressure is relatively small [40]. Nevertheless, at very small distances the deviations of the surface of liquid from the horizontal level can be significant. However, such small distances are not considered here. For small and slowly changing slopes of the surface, the solutions obtained by Moffatt, Eqs. (9)–(12), can be used as approximate solutions with the angle ϕ depending on the local slope [37,71].

Surfactant balance at the surface

The solution of the hydrodynamic problem presented above is based on the assumption of a specific surfactant distribution at the meniscus surface, namely, a separation of the meniscus surface on the mobile and immobile parts with a sharp transition between them. On the other side, the surfactant distribution at the surface should be described by the balance equation, Eq. (6), or its dimensionless form, Eq. (8f). According to Eq. (8f), the surfactant distribution is determined by the dimensionless Péclet numbers Pe and Pe_s and the dimensionless number N_E . To estimate these numbers, we have to choose a characteristic length scale L . This can be, for example, the capillary length λ_C or, what is more suitable for the considered here problem, the size of the surfactant free zone, x_0 , which can change, however, in rather wide limits, according to Eq. (26) or (27). Let us assume, that the characteristic length scale, L , changes between 1 μ m and 1 mm. Then, for the substrate velocity of about 10 cm/s and the diffusion coefficient of about 10^{-10} m²/s, we obtain the surface Péclet numbers $Pe_s \sim 10^3$ to 10^6 . Thus, the contribution of surface diffusion to the surfactant distribution should be small as it is proportional to $(Pe_s)^{-1}$.

The surfactant adsorption (or desorption) from the bulk solution is described by the last term in Eq. (8f), which is inversely proportional to $Pe/N_E = U(\Gamma_{eq}/c_{eq})/D$. The coefficient Pe/N_E has a sense of a Péclet number defined with the characteristic length scale $L = \Gamma_{eq}/c_{eq}$, which characterizes the adsorption activity of the surfactant (sometimes it is called “adsorption length”). This parameter can change in very wide limits, but for typical surfactants $\Gamma_{eq}/c_{eq} \sim 10^{-6}$ to 10^{-3} m. Then, for the same other parameters, we obtain $Pe/N_E \sim 10^3$ to 10^6 , i.e., it is in the same range as the surface Péclet number, estimated above. Thus, for the considered conditions,

the influence of the surfactant exchange with the bulk solution should be also small.

By neglecting the surface diffusion and surfactant exchange with the bulk solution, under steady-state conditions, Eq. (8f) takes the form

$$\tilde{\nabla}_s(\tilde{\Gamma}\tilde{u}_s) \approx 0 \quad (30)$$

This means that the surfactant convective flux should be approximately constant at the surface for the considered wedge geometry: $\tilde{J}_C = \tilde{\Gamma}\tilde{u}_s \approx const$. This constant flux should be equal to the flux of surfactant molecules desorbed from the substrate (rotating cylinder) surface at the contact line, when it leaves the solution. If the surfactant molecules do not desorb from the substrate surface, then $J_C \approx 0$, and we have

$$\tilde{\Gamma}\tilde{u}_s \approx 0 \quad (31)$$

This equation is satisfied, if either $\tilde{\Gamma} \approx 0$ (for mobile part of the surface $r < r_0$), or $u_s \approx 0$ (for immobile part of the surface $r_0 > r$) [55,56,61,63]. Such consideration assumes an infinitely small transition region between the mobile and immobile parts of the surface, what is not realized in practice. In real systems the surface diffusion and surfactant exchange with the bulk solution make the transition region more diffuse and not so sharp.

If the surface diffusion is active, then instead of Eq. (30) we have

$$\tilde{\nabla}_s(\tilde{\Gamma}\tilde{u}_s) - \frac{1}{Pe_s}\tilde{\Delta}_s\tilde{\Gamma} = 0 \quad (32)$$

This equation describes a convective-diffusion problem with a high Péclet number. In such situations, the convective solute transfer prevails everywhere in the system except of a thin boundary layer (transition zone between the mobile and immobile parts of the surface). The thickness of such diffusion boundary layer is inversely proportional to the Péclet number $\delta \sim (Pe_s)^{-1}$. Because of a small boundary layer thickness, the concentration gradient in this layer is strong enough to compensate the convective solute transfer under steady-state conditions. Note, a small transition layer thickness is a precondition for the applicability of the models in the previous sections with a clear separation between the mobile and immobile parts.

For the transition layer, the longitudinal coordinate in Eq. (32) can be renormalized by using $\tilde{\delta}_s = L \cdot (Pe_s)^{-1}$ as a new scaling factor: $\tilde{r}' = \tilde{r}Pe_s$ (or $\tilde{x}' = \tilde{x}Pe_s$). With this

new dimensionless coordinate, the small multiplier $(Pe_s)^{-1}$ before the second term in Eq. (32) disappears. This means that the increase of the dimensionless adsorption $\tilde{\Gamma}$ within this thin layer is of the order of unit, i.e. practically all increase of the adsorption should happen here, and the remaining part of the mobile zone at the surface is almost clean of surfactants.

When the surfactant adsorption and desorption are significant then we similarly have

$$\tilde{\nabla}_s(\tilde{\Gamma}\tilde{u}_s) + \frac{N_E}{Pe} \left(\frac{\partial \tilde{c}}{\partial \tilde{n}} \right)_s = 0 \quad (33)$$

The last term in this equation depends on the surfactant distribution in the bulk, which is described by a stationary convective diffusion equation

$$\tilde{\mathbf{u}} \cdot \tilde{\nabla} \tilde{c} - \frac{1}{Pe} \tilde{\Delta} \tilde{c} = 0 \quad (34)$$

In our case, the transversal diffusion near the surface is much more significant than the longitudinal one; therefore, we can write

$$\tilde{u}_x \frac{\partial \tilde{c}}{\partial \tilde{x}} - \frac{1}{Pe} \frac{\partial^2 \tilde{c}}{\partial \tilde{y}^2} = 0 \quad (35)$$

where \tilde{x} and \tilde{y} are local Cartesian coordinates. This equation describes the situation, when a diffusion boundary layer forms in the solution under the free moving surface. The thickness of this boundary layer is inversely proportional to \sqrt{Pe} : $\delta_D \sim 1/\sqrt{Pe}$ [22,60,83]. The transversal coordinate in Eq. (35) can be also renormalized by using $\delta_D = L/\sqrt{Pe}$ as a new scaling factor: $\tilde{y}' = \tilde{y}\sqrt{Pe}$. Then, within the thin boundary layer the two terms in Eq. (35) will have the same order of magnitude. Thus, the transversal concentration gradient is determined by the thickness of this boundary layer, and this should be accounted for in Eq. (33):

$$\frac{\partial}{\partial \tilde{x}} (\tilde{\Gamma}\tilde{u}_x) + \frac{N_E}{\sqrt{Pe}} \left(\frac{\partial \tilde{c}}{\partial \tilde{y}'} \right)_{\tilde{y}'=0} = 0 \quad (36)$$

Integration of this equation shows that the dimensionless convective surfactant flux should be of the order

$$\tilde{J}_C = \tilde{\Gamma}\tilde{u}_x \sim \frac{N_E}{\sqrt{Pe}} \int_0^1 \left(\frac{\partial \tilde{c}}{\partial \tilde{y}'} \right)_{\tilde{y}'=0} d\tilde{x} \quad (37)$$

As the integral in this equation is of the order of unity (because of the scaling reasons), then the dimensionless convective flux is of the order of $\tilde{J}_C \sim N_E/\sqrt{Pe}$. Hence,

the convective flux in the mobile part of the surface will be small, if $N_E/\sqrt{Pe} \ll 1$. For $L \sim 1$ mm, $U \sim 10$ cm/s and $D \sim 10^{-10}$ m²/s the Péclet number is $Pe \sim 10^6$. For less soluble (but more surface active) surfactants $\Gamma_{eq}/c_{eq} \sim 10^{-3}$ m, therefore, the convective flux is small: $N_E/\sqrt{Pe} \sim 10^{-3}$. For better soluble (but less surface active) surfactants, we can have $\Gamma_{eq}/c_{eq} \sim 10^{-6}$ m and $N_E/\sqrt{Pe} \sim 1$.

Thus, the situation with separation of the meniscus surface onto mobile and immobile part is expected for less soluble surfactants (having larger Γ_{eq}/c_{eq} ratios), because in this case, the convective flux in the mobile part of the surface should be small, and the amount of surfactant in this part should be also small. The transition zone between the mobile and immobile part should be small, as defined by surface diffusion. The diffusion and adsorption of perfectly soluble (but low surface active) surfactants is much faster; therefore, they can adsorb in sufficiently large amounts in the mobile part, making it only partially mobile. In this case, the transition zone between the mobile and immobile part should be smoother and wider, and the proposed here model (developed for surfactants with low CMC values) can be not applicable. If there is a kinetic adsorption barrier, then the rate of adsorption will be smaller, and the transition zone between the mobile and immobile part will be sharper.

The surfactant molecules adsorbed at the mobile part are continuously swept joining to the surfactant accumulated in the immobile part. Thus, under stationary conditions, the dynamic adsorption layer in the immobile part should shift slowly out from the contact line. That means, this layer is not completely immobile. But for low soluble surfactants, the rate of adsorption is small, and the shift of the adsorption layer within the immobile part should be also very slow. In this case, when solving the hydrodynamic problem, it can be considered as immobile. For insoluble surfactants, this should be a rigorous assumption.

However, this assumption can be violated, if a significant part of surfactant molecules desorb from the substrate at the contact line. These desorbed molecules are a part of the convective flux at the mobile part of the surface and support the slow shift of the dynamic adsorption layer in the immobile part. Therefore, the difference between the velocities in the mobile and immobile part can be significant, if only a small part of the surfactant molecules desorb from the substrate surface while it leaves the solution, so that the surface concentration in the mobile part remains much smaller than in the immobile part.

If there is a slow shift of the adsorption layer within the immobile part, then the excess of surfactant should desorb far away from the meniscus. Under steady-state

conditions, the amount of the surfactant adsorbed in the mobile part (or coming to the liquid surface from the substrate surface) should be equal to the amount desorbed from the liquid surface in distant parts of the solution. Therefore, in the immobile part, the surfactant adsorption should be slightly above the equilibrium adsorption, and the surface tension should be slightly below the equilibrium surface tension. This can lead, in particular, to long-range transport processes (like diffusion and advection) between the different regions at the solution surface in the vessel [68]. However, under typical experimental conditions, the area of the solution surface is usually much larger than the meniscus area. Then the desorption should take a place from a much larger surface than the surface, where the adsorption occurs within the meniscus region. Accordingly, the surface tension in distant parts of the solution should be only slightly below the equilibrium one to ensure a sufficiently high desorption flux, as it was discussed at the beginning.

These considerations show that while the size of the mobile part is controlled by the equilibrium surface pressure $\Pi = \gamma_0 - \gamma_{eq}$ (or the Marangoni number, Eqs. (25)-(27)), the steepness of the surface tension gradient within the transition zone between the mobile and immobile parts is determined by the adsorption activity of the surfactant and the rate of surface diffusion.

As it was discussed at the beginning, the peculiarities of the surfactant distribution at the surface should influence the velocity and viscous stress distributions. In this respect, it is quite reasonable to assume that the steepness of the surface tension gradient within the transition zone should have effect on the viscous stress peaks at the leading edge of the immobile part of the surface. The viscous stress peaks presented in Figure 6a are very sharp because they were obtained under the assumption of a negligibly small transition zone and a very steep surface tension gradient between the mobile and immobile parts. The higher are the adsorption activity of the surfactant and the rate of surface diffusion, the smoother is the surface tension gradient within the transition zone, and the viscous stress peaks should become less sharp. The same is observed for bubbles rising in surfactant solutions where the rear part of the bubble is retarded by the adsorbed surfactant molecules [56].

Conclusions

The liquid velocity profiles in a steady dewetting meniscus have been analyzed from the hydrodynamic and convective diffusion points of view by taking into account possible viscous stresses variations and non-uniform retardation of the meniscus surface due to the presence of a dynamic adsorption layer. It has been shown that the solutions of the hydrodynamic problem obtained by Moffatt [77] give accurate velocity profiles

in the two limiting cases of a completely free or completely retarded meniscus surface. However, in surfactant solutions with small concentrations, a non-uniform retardation of the meniscus surface is expected, where the available analytical solutions are not applicable. With increasing flow velocity, the non-uniformity of the meniscus surface retardation becomes stronger, and a separation of the surface on a mobile and an immobile part with a sharp transition between them is possible. Near the transition point, the velocity profiles change sharply, and the viscous stresses strongly increase in this region. A very similar separation of the surface on a mobile and an immobile part is observed also at the surface of rising bubbles or rising/falling drops in surfactant solutions and in other surfactants containing systems with similar flow conditions.

The surface tension gradients, which are a consequence of the tangential viscous stresses acting at the surfactant covered surface, start to form and retard the part of the surface further away from the transition point. The numerical calculations of the flow profiles allow to obtain a logarithmic decrement for the surface tension variation with increasing distance from the contact line. This decrement is close to that calculated by using the Moffatt solution [77], except a small region near the transition point, where the surface tension has a rather small initial decrease. With this decrement, the surface tension difference required to immobilize the surface can be calculated. If the equilibrium surface pressure for the considered surfactant solution exceeds, this required surface tension difference, then the solution surface should be completely immobilized by the Marangoni stresses. However, if the surfactant concentration in the solution is small, the Marangoni stresses can be insufficient to counteract the tangential viscous stresses at the surface. In this case, a mobile part can appear at the surface, where the adsorbed surfactant molecules are swept toward the retarded part of the surface. The size of this mobile part is determined by the dimensionless Marangoni number and the surface pressure. The mobile part becomes broader, when the flow velocity or the solution viscosity increases or the equilibrium surface pressure decreases.

The balance at the surface is determined by the rate of convective transfer, diffusion, and adsorption rate of the solution components. In the dimensionless form, the surfactant balance is expressed through the bulk and surface Péclet numbers and the adsorption activity coefficient. The analysis shows that the size of the transition zone between the mobile and immobile parts of the surface is determined by surface diffusion, whereas the difference in surface mobility between these two parts is determined by the solubility of the solution components. For less soluble surfactants, the difference in surface mobility should be much more significant than for more soluble. The kinetic adsorption barrier

should be in favor of a more significant difference, while the surfactant desorption from the substrate surface should reduce the difference.

The obtained results show that the flow profiles near the contact line can be modified due to surfactants presence. The meniscus surface can be immobilized, fully or partially, and up to different distances from the contact line, depending on the particular conditions. For different flow profiles the hydrodynamic energy dissipation within the dynamic meniscus should be different. This should lead to a dependence of the dynamic contact angle on the surfactant concentration. In particular, besides the apparent contact angle for zero velocity, the friction parameter in the hydrodynamic theory can be influenced by the surfactants [66]. However, the most significant part of energy dissipates on small distances from the contact line, where the considered here model cannot be applied. Therefore, a more general model is necessary to analyze quantitatively the effect of surfactants on the dynamic contact angle.

Declaration of competing interest

The authors declare the following financial interests/ personal relationships which may be considered as potential competing interests:

V.I.Kovalchuk reports financial support was provided by European Commission. V.I.Kovalchuk reports financial support was provided by National Research Foundation of Ukraine. V.I.Kovalchuk reports financial support was provided by German Academic Exchange Service. G.K. Auernhammer reports financial support was provided by German Research Foundation.

Data availability

No data was used for the research described in the article.

Acknowledgements

We gratefully acknowledge the financial support by the Deutsche Forschungsgemeinschaft – Project-ID 265191195 – SFB 1194 (GKA), by European Commission within the scope of FP Horizon 2020 (Project “EHAWEDRY”, Grant Agreement No. 964524) (VIK) and National Research Foundation of Ukraine (project number 2020.02/0138) (VIK). A fellowship of the DAAD (VIK) is also gratefully acknowledged.

Appendix A. Supplementary data

Supplementary data to this article can be found online at <https://doi.org/10.1016/j.cocis.2023.101723>.

References

Papers of particular interest, published within the period of review, have been highlighted as:

- * of special interest
- ** of outstanding interest

1. Rosen MJ, Kunjappu JT: *Surfactants and interfacial phenomena*. 4th ed. Hoboken: Wiley; 2012.

2. Romsted L (Ed.). *Surfactant science and technology: retrospects and prospects*. Boca Raton: CRC Press/Taylor and Francis Group; 2014.
3. Bonn D, Eggers J, Indekeu J, Meunier J, Rolley E: **Wetting and spreading**. *Rev Mod Phys* 2009, **81**:739–805, <https://doi.org/10.1103/RevModPhys.81.739>.
4. Ralston J, Dukhin SS, Mishchuk NA: **Wetting film stability and flotation kinetics**. *Adv Colloid Interface Sci* 2002, **95**:145–236, [https://doi.org/10.1016/s0001-8686\(00\)00083-x](https://doi.org/10.1016/s0001-8686(00)00083-x).
5. Kovalchuk NM, Simmons MJH: **Surfactant-mediated wetting and spreading: recent advances and applications**. *Curr Opin Colloid Interface Sci* 2020, **51**:101375, <https://doi.org/10.1016/j.cocis.2020.07.004>.
6. Gaines Jr GL: *Insoluble monolayers at liquid–gas interfaces*. New York: Wiley-Interscience; 1966.
7. Langevin D, Monroy F: **Interfacial rheology of polyelectrolytes and polymer monolayers at the air-water interface**. *Curr Opin Colloid Interface Sci* 2010, **15**:283–293, <https://doi.org/10.1016/j.cocis.2010.02.002>.
8. Fainerman VB, Möbius D, Miller R: **Surfactants – chemistry, interfacial properties, applications**. In *Studies in Interface Science*, 13. Elsevier; 2001.
9. Schramm LL: *Surfactants: fundamentals and applications in the petroleum industry*. Cambridge University Press; 2010.
10. Sjöblom J: *Encyclopedic handbook of emulsion technology*. New York, NY: Marcel Dekker Inc.; 2001.
11. Kistler SF, Schweizer PM: *Liquid film coating: scientific principles and their technological implications*. London: Chapman & Hall; 1997.
12. Nguyen AV, Schulze HJ: **Colloidal science of flotation**. In *Surfactant science ser*, **118**. New York: Marcel Dekker; 2004.
13. **Microfluidics based microsystems**. In *NATO science for peace and security series A: chemistry and biology*. Edited by Kakaç S, Kosoy B, Li D, Pramuanjaroenkij A, Dordrecht: Springer; 2010.
14. Javadi A, Krägel J, Kovalchuk VI, Liggieri L, Loglio G, Aksenenko EV, Fainerman VB, Miller R: **Dynamics of interfacial layer formation**. In Rahni MT, Karbaschi M, Miller R. *Progress in colloid and interface science*, **5**. Boca Raton: CRC Press/Taylor & Francis Group; 2016:83–104. Computational Methods for Complex Liquid-Fluid Interfaces.
15. Lotfi M, Karbaschi M, Javadi A, Mucic N, Krägel J, Kovalchuk VI, Rubio RG, Fainerman VB, Miller R: **Dynamics of liquid interfaces under various types of external perturbations**. *Curr Opin Colloid Interface Sci* 2014, **19**:309–319, <https://doi.org/10.1016/j.cocis.2014.04.006>.
16. Yopez C, Naude J, Méndez F: **Physical impact of a surfactant on the nonlinear oscillations of a microbubble considering a dynamic surface tension and subject to an external acoustic field**. *Phys. Rev. Fluids* 2022, **7**:63603, <https://doi.org/10.1103/PhysRevFluids.7.063603>.
17. Straub BB, Schmidt H, Rostami P, Henrich F, Rossi M, Kähler CJ, *et al.*: **Flow profiles near receding three-phase contact lines: influence of surfactants**. *Soft Matter* 2021, **17**:10090, <https://doi.org/10.1039/D1SM01145F>.
- In this work the quantitatively measured flow profiles near receding contact lines in surfactant solutions are compared to modeling considerations of 2D models. The authors found hints for effects of a 3D flow profile in the drop.
18. Kovalchuk NM, Simmons MJH: **Effect of soluble surfactant on regime transitions at drop formation**. *Colloids Surf, A* 2018, **545**:1–7, <https://doi.org/10.1016/j.colsurfa.2018.02.041>.
19. Liu C-Y, Carvalho MS, Kumar S: **Mechanisms of dynamic wetting failure in the presence of soluble surfactants**. *J Fluid Mech* 2017, **825**:677–703, <https://doi.org/10.1017/jfm.2017.394>.
20. Dukhin SS, Kretschmar G, Miller R: **Dynamics of adsorption at liquid interfaces: theory, experiment, application**. In Möbius D, Miller R. *Studies of interface science*, **1**. Amsterdam: Elsevier; 1995.

21. Manikantan H, Squires TM: **Surfactant dynamics: hidden variables controlling fluid flows**. *J Fluid Mech* 2020, **892**:P1, <https://doi.org/10.1017/jfm.2020.170>.
- An important review paper summarizing the most significant results related to a coupling between hydrodynamic processes and physico-chemical processes in liquid systems containing surfactants.
22. Levich VG: *Physicochemical hydrodynamics*. Englewood Cliffs, NJ: Prentice-Hall; 1962.
23. Edwards DA, Brenner H, Wasan DT: *Interfacial transport processes and rheology*. Stonham, Massachusetts: Butterworth-Heinemann; 1991.
24. Kovalchuk VI, Kamusewitz H, Vollhardt D, Kovalchuk NM: **Auto-oscillation of surface tension**. *Phys Rev E* 1999, **60**: 2029–2036, <https://doi.org/10.1103/PhysRevE.60.2029>.
25. Schwarzenberger K, Köllner T, Linde H, Boeck T, Odenbach S, Eckert K: **Pattern formation and mass transfer under stationary solutal Marangoni instability**. *Adv Colloid Interface Sci* 2014, **206**:344–371, <https://doi.org/10.1016/j.cis.2013.10.003>.
26. Kovalchuk VI, Zholkovskiy EK, Bondarenko MP, Vollhardt D: **Wetting instabilities in Langmuir-Blodgett film deposition**. In *Surfactant science and technology: retrospects and prospects*. Edited by Romsted L, P 193-212, Boca Raton: CRC Press/Taylor and Francis Group; 2014.
27. Cox RG: **The dynamics of the spreading of liquids on a solid surface. 1. Viscous flow**. *J Fluid Mech* 1986, **168**:169–194, <https://doi.org/10.1017/S0022112086000332>.
28. Voinov OV: **Meniscus contact angle in unsteady viscous flow**. *J Colloid Interface Sci* 1998, **201**:93–102, <https://doi.org/10.1006/jcis.1997.5371>.
29. Blake TD, Haynes JM: **Kinetics of liquid/liquid displacement**. *J Colloid Interface Sci* 1969, **30**:421–423, [https://doi.org/10.1016/0021-9797\(69\)90411-1](https://doi.org/10.1016/0021-9797(69)90411-1).
30. Blake TD: **The physics of moving wetting lines**. *J Colloid Interface Sci* 2006, **299**:1–13, <https://doi.org/10.1016/j.jcis.2006.03.051>.
31. Starov VM, Velarde MG: *Wetting and spreading dynamics*. 2nd ed. Boca Raton: CRC Press/Taylor and Francis Group; 2020.
32. Gupta C, Dora LC, Dixit HN: **An experimental study of flow patterns near a moving contact line**. In 11th international Conference on multiphase flow (ICMF 2023) April 2–7; 2023. Kobe, Japan, http://www.jsmf.gr.jp/icmf2022/doc/program_final.pdf; 2023.
33. Blake TD, Fernández-Toledano J-C, De Coninck J: **A possible way to extract the dynamic contact angle at the molecular scale from that measured experimentally**. *J Colloid Interface Sci* 2023, **629**:660–669, <https://doi.org/10.1016/j.jcis.2022.08.170>.
34. Fernández-Toledano J-C, Blake TD, De Coninck J: **Moving contact lines and Langevin formalism**. *J Colloid Interface Sci* 2020, **562**:287–292, <https://doi.org/10.1016/j.jcis.2019.11.123>.
35. Fan JC, De Coninck J, Wu HA, Wang FC: **A generalized examination of capillary force balance at contact line: on rough surfaces or in two-liquid systems**. *J Colloid Interface Sci* 2021, **585**:320–327, <https://doi.org/10.1016/j.jcis.2020.11.100>.
36. Cox RG: **The dynamics of the spreading of liquids on a solid surface. 2. Surfactants**. *J Fluid Mech* 1986, **168**:195–220, <https://doi.org/10.1017/S0022112086000344>.
- This is a thorough theoretical analysis of the dynamics of the spreading of liquids on a solidsurface. The possibility of formation of surfactant free regions on the surface of liquid menisci under dynamic conditions in surfactant containing liquids was predicted.
37. Chesters AK, Elyousfi ABA: **The influence of surfactants on the hydrodynamics of surface wetting. I. The nondiffusing limit**. *J Colloid Interface Sci* 1998, **207**:20–29, <https://doi.org/10.1006/jcis.1998.5705>.
38. Elyousfi ABA, Chesters AK, Cazabat AM, Villette S: **Approximate solution for the spreading of a droplet on a smooth solid surface**. *J Colloid Interface Sci* 1998, **207**:30–40, <https://doi.org/10.1006/jcis.1998.5706>.
39. Fuentes J, Cerro RL: **Surface forces and inertial effects on moving contact lines**. *Chem Eng Sci* 2007, **62**:3231–3241, <https://doi.org/10.1016/j.ces.2007.03.012>.
40. Huh C, Scriven LE: **Hydrodynamic model of the steady movement of a solid/liquid/fluid contact line**. *J Colloid Interface Sci* 1971, **35**:85–101, [https://doi.org/10.1016/0021-9797\(71\)90188-3](https://doi.org/10.1016/0021-9797(71)90188-3).
41. Blake TD, Shikhmurzaev YD: **Dynamic wetting by liquids of different viscosity**. *J Colloid Interface Sci* 2002, **253**:196–202, <https://doi.org/10.1006/jcis.2002.8513>.
42. Shikhmurzaev YD: **The moving contact line on a smooth solid surface**. *Int J Multiphas Flow* 1993, **19**:589–610, [https://doi.org/10.1016/0301-9322\(93\)90090-H](https://doi.org/10.1016/0301-9322(93)90090-H).
43. Sprittles JE, Shikhmurzaev YD: **Finite element simulation of dynamic wetting flows as an interface formation process**. *J Comput Phys* 2013, **233**:34–65, <https://doi.org/10.1016/j.jcp.2012.07.018>.
44. Billingham J: **On a model for the motion of a contact line on a smooth solid surface**. *Eur J Appl Math* 2006, **17**:347–382, <https://doi.org/10.1017/S0956792506006589>.
45. Jin F, Gupta NR, Stebe KJ: **The detachment of a viscous drop in a viscous solution in the presence of a soluble surfactant**. *Phys Fluids* 2006, **18**:22103, <https://doi.org/10.1063/1.2172003>.
46. Fleckenstein S, Bothe D: **Simplified modeling of the influence of surfactants on the rise of bubbles in VOF-simulations**. *Chem Eng Sci* 2013, **102**:514–523, <https://doi.org/10.1016/j.ces.2013.08.033>.
47. Hosokawa S, Masukura Y, Hayashi K, Tomiyama A: **Experimental evaluation of Marangoni stress and surfactant concentration at interface of contaminated single spherical drop using spatiotemporal filter velocimetry**. *Int J Multiphas Flow* 2017, **97**:157–167, <https://doi.org/10.1016/j.ijmultiphaseflow.2017.08.007>.
48. Hosokawa S, Hayashi K, Tomiyama A: **Evaluation of adsorption of surfactant at a moving interface of a single spherical drop**. *Exp Therm Fluid Sci* 2018, **96**:397–405, <https://doi.org/10.1016/j.expthermflusci.2018.03.026>.
- The authors measured the velocity and viscous stress distributions and evaluated the molar flux of surfactant to the interface for spherical drops falling in a stagnant liquid containing surfactant.
49. Bastani D, Fayzi P, Lotfi M, Arzideh SM: **CFD simulation of bubble in flow field: investigation of dynamic interfacial behaviour in presence of surfactant molecules**. *Colloid Interface Sci Comm* 2018, **27**:1–10, <https://doi.org/10.1016/j.colcom.2018.09.001>.
50. Danov KD, Valkovska DS, Ivanov IB: **Effect of surfactants on the film drainage**. *J Colloid Interface Sci* 1999, **211**:291–303, <https://doi.org/10.1006/jcis.1998.5973>.
51. Bhamla MS, Giacomini CE, Balemans C, Fuller GG: **Influence of interfacial rheology on drainage from curved surfaces**. *Soft Matter* 2014, **10**:6917–6925, <https://doi.org/10.1039/C3SM52934G>.
52. Kovalchuk VI, Krägel J, Pandolfini P, Loglio G, Liggieri L, Ravera F, Makievski AV, Miller R: **dilatational rheology of thin liquid films**. In Miller R, Liggieri L. *Interfacial rheology*, Progress in Colloid and interface science, **1**. Leiden-Boston: Brill; 2009:476–518.
53. Lucassen-Reynders EH, Lucassen J: **Surface dilatational rheology: past and present**. In Miller R, Liggieri L. *Interfacial rheology*, Progress in Colloid and interface science, **1**. Leiden-Boston: Brill; 2009:38–76.
54. Sundin J, Bagheri S: **Slip of submerged two-dimensional liquid-infused surfaces in the presence of surfactants**. *J Fluid Mech* 2022, **950**:A35, <https://doi.org/10.1017/jfm.2022.835>.
55. Bel Fdhila R, Duineveld PC: **The effect of surfactant on the rise of a spherical bubble at high Reynolds and Peclet numbers**. *Phys Fluids* 1996, **8**:310–321, <https://doi.org/10.1063/1.868787>.
56. Cuenot B, Magnaudet J, Spennato B: **The effects of slightly soluble surfactants on the flow around a spherical bubble**.

- J Fluid Mech* 1997, **339**:25–53, <https://doi.org/10.1017/S0022112097005053>.
57. Zhang Y, McLaughlin JB, Finch JA: **Bubble velocity profile and model of surfactant mass transfer to bubble surface.** *Chem Eng Sci* 2001, **56**:6605–6616, [https://doi.org/10.1016/S0009-2509\(01\)00304-9](https://doi.org/10.1016/S0009-2509(01)00304-9).
58. Malysa K, Krasowska M, Krzan M: **Influence of surface active substances on bubble motion and collision with various interfaces.** *Adv Colloid Interface Sci* 2005, **114**:205–225, <https://doi.org/10.1016/j.cis.2004.08.004>.
59. Krzan M, Zawala J, Malysa K: **Development of steady state adsorption distribution over interface of a bubble rising in solutions of n-alkanols (C5, C8) and n-alkyl-trimethylammonium bromides (C8, C12, C16).** *Colloids Surf, A* 2007, **298**:42–51, <https://doi.org/10.1016/j.colsurfa.2006.12.056>.
The profiles of the bubble local velocity in various surfactant solutions are measured and adsorption distributions over the interface of rising bubbles are analyzed.
60. Dukhin SS, Kovalchuk VI, Gochev GG, Lotfi M, Krzan M, Malysa K, Miller R: **Dynamics of Rear Stagnant Cap formation at the surface of spherical bubbles rising in surfactant solutions at large Reynolds numbers under conditions of small Marangoni number and slow sorption kinetics.** *Adv Colloid Interface Sci* 2015, **222**:260–274, <https://doi.org/10.1016/j.cis.2014.10.002>.
In this paper the experimental and theoretical results on a non-steady process of bubble rising in surfactant solutions are summarized. The kinetics of growth of the Rear Stagnant Cap is analyzed.
61. Sadhal SS, Johson RE: **Stokes flow past bubbles and drops partially coated with thin films. Part 1. Stagnant cap of surfactant film - exact solution.** *J Fluid Mech* 1983, **126**:237–250, <https://doi.org/10.1017/S0022112083000130>.
62. He Z, Maldarelli C, Dagan Z: **The size of stagnant caps of bulk soluble surfactant on the interfaces of translating fluid droplets.** *J Colloid Interface Sci* 1991, **146**:442–451, [https://doi.org/10.1016/0021-9797\(91\)90209-Q](https://doi.org/10.1016/0021-9797(91)90209-Q).
63. McLaughlin JB: **Numerical simulation of bubble motion in water.** *J Colloid Interface Sci* 1996, **184**:614–625, [https://doi.org/10.1016/S0009-2509\(99\)00412-1](https://doi.org/10.1016/S0009-2509(99)00412-1).
64. Zholkovskij EK, Koval'chuk VI, Dukhin SS, Miller R: **Dynamics of rear stagnant cap formation at low Reynolds numbers. 1. Slow sorption kinetics.** *J Colloid Interface Sci* 2000, **226**:51–59, <https://doi.org/10.1006/jcis.2000.6786>.
65. Harper JF: **The leading edge of an oil slick, soap film, or bubble stagnant cap in Stokes flow.** *J Fluid Mech* 1992, **237**:23–32, <https://doi.org/10.1017/S0022112092003331>.
66. Henrich F, Fell D, Truskowska D, Weirich M, Anyfantakis M, Nguyen T-H, Wagner M, Auernhammer GK, Butt H-J: **Influence of surfactants in forced dynamic dewetting.** *Soft Matter* 2016, **12**:7782–7791, <https://doi.org/10.1039/C6SM00997B>.
The dynamic receding contact angles are measured with the rotating cylinder setup for several surfactants of different type and solubility. It is shown that the dynamic receding contact angles versus concentrations of surfactants in % of CMC are similar for surfactants with very different CMC values.
67. Fell D, Auernhammer G, Bonaccorso E, Liu C, Sokuler R, Butt H-J: **Influence of surfactant concentration and background salt on forced dynamic wetting and dewetting.** *Langmuir* 2011, **27**:2112–2117, <https://doi.org/10.1021/la104675t>.
68. Fell D, Pawanrat N, Bonaccorso E, Butt H-J, Auernhammer GK: **Influence of surfactant transport suppression on dynamic contact angle hysteresis.** *Colloid Polym Sci* 2013, **291**:361–366, <https://doi.org/10.1007/s00396-012-2759-y>.
69. Eibach TF, Fell D, Nguyen H, Butt H-J, Auernhammer GK: **Measuring contact angle and meniscus shape with a reflected laser beam.** *Rev Sci Instrum* 2014, **85**:13703, <https://doi.org/10.1063/1.4861188>.
70. Truskowska D, Henrich F, Schultze J, Koynov K, Räder HJ, Butt H-J, Auernhammer GK: **Forced dewetting dynamics of high molecular weight surfactant solutions.** *Colloids Surf, A* 2017, **521**:30–37, <https://doi.org/10.1016/j.colsurfa.2016.07.073>.
71. Voinov OV: **Hydrodynamics of wetting.** *Fluid Dynam* 1976, **11**:714–721, <https://doi.org/10.1007/BF01012963>.
72. Eggers J: **Existence of receding and advancing contact lines.** *Phys Fluids* 2005, **17**:82106, <https://doi.org/10.1063/1.2009007>.
73. Chan TS, Gueudre T, Snoeijer JH: **Maximum speed of dewetting on a fiber.** *Phys Fluids* 2011, **23**:112103, <https://doi.org/10.1063/1.3659018>.
74. Petrov PG, Petrov JG: **A combined molecular-hydrodynamic approach to wetting kinetics.** *Langmuir* 1992, **8**:1762–1767, <https://doi.org/10.1021/la00043a013>.
75. Butt H-J, Berger R, Steffen W, Vollmer D, Weber SAL: **Adaptive wetting – adaptation in wetting.** *Langmuir* 2018, **34**:11292–11304, <https://doi.org/10.1021/acs.langmuir.8b01783>.
The authors critically discuss different types of adaptation in wetting processes, give clear and concise descriptions and provide a simple modeling in terms of a relaxation model.
76. Fainerman VB, Miller R, Aksenenko EV, Makievski AV: **Equilibrium adsorption properties of single and mixed surfactant solutions – chemistry, interfacial properties, applications.** Edited by Fainerman VB, Möbius D, Miller R, *Studies in interface science*, **13**. Amsterdam: Elsevier; 2001:189–285.
77. Moffatt HK: **Viscous and resistive eddies near a sharp corner.** *J Fluid Mech* 1964, **18**:1–18, <https://doi.org/10.1017/S0022112064000015>.
In this paper the solutions of the hydrodynamic problem for the flow near a corner for two important limiting cases are given, when either the viscous stresses are zero at the surface (for solution free of surfactants) or the surface is fully retarded by the adsorbed surfactants.
78. Taylor GI: **On scraping viscous fluid from a plane surface.** In *Miszellangen der angewandten mechanik (festschrift walter tollmien)*. Edited by Schäfer M, **315**. Berlin: Akademie-Verlag; 1962:313.
79. Kuhlmann HC, Nienhüser C, Rath HJ: **The local flow in a wedge between a rigid wall and a surface of constant shear stress.** *J Eng Math* 1999, **36**:207–218, <https://doi.org/10.1023/A:1004547203342>.
80. Mahmood A, Siddiqui AM: **Two dimensional inertial flow of a viscous fluid in a corner.** *Appl Math Sci* 2017, **11**:407–424, <https://doi.org/10.12988/ams.2017.612282>.
81. Lucassen J: **Dynamic properties of free liquid films and foams.** In *Anionic surfactants. Physical chemistry of surfactant action*. Edited by Lucassen-Reynders EH, **11**. NY: Marcel Dekker Inc; 1981:217–265. Surfactant Science Ser.
82. de Gennes PG: **Deposition of Langmuir-Blodgett layers.** *Colloid Polym Sci* 1986, **264**:463–465, <https://doi.org/10.1007/BF01419552>.
83. Ulaganathan V, Krzan M, Lotfi M, Dukhin SS, Kovalchuk VI, Javadi A, Gunes DZ, Gehin-Delval C, Malysa K, Miller R: **Influence of β -lactoglobulin and its surfactant mixtures on velocity of the rising bubbles.** *Colloids Surf, A* 2014, **460**:361–368, <https://doi.org/10.1016/j.colsurfa.2014.04.041>.